Kinetics of the Direct Sulfation of Limestone at the Initial Stage of Crystal Growth of the Solid Product

Guilin Hu, Kim Dam-Johansen, and Stig Wedel
CHEC, Dept. of Chemical and Biochemical Engineering, Technical University of Denmark, 2800 Lyngby, Denmark

DOI 10.1002/aic.12363
Published online August 12, 2010 in Wiley Online Library (wileyonlinelibrary.com).

The direct sulfation of limestone was studied in a quartz bench scale fixed-bed reactor with the technique of data deconvolution. The obtained results show that the direct sulfation of limestone has a two-period kinetic behavior: a short initial sulfation period with high but fast decreasing reaction rate and a subsequent period with product crystal growth with low-conversion rate. The transition from the first period to the second period is sharp and indicates clearly the start point of the period with product crystal growth. The transition point was determined by the concentrations of gases such as SO_2, O_2, and CO_2 and the temperature. The sulfation process in the initial stage of the period with product crystal growth can be described by the combination of the sulfation reaction at the gas–solid interface, diffusion of the product ions toward the product crystal grains, diffusion of carbonate ions toward the gas–solid interface to react, and the gradual shielding of calcite surface area by the product crystal grains. A simple and semi-empirical mathematical model derived on basis of this theory gives a satisfactory description of the experimental results up to a calcite conversion of about 0.5%. © 2010 American Institute of Chemical Engineers *AIChE J,* 57: 1607–1616, 2011
Keywords: sulfation, limestone, kinetics, modeling, SO_2, desulfurization, crystal growth

Introduction

Limestone is a frequently used sorbent for the desulfurization of industrial flue gases at elevated temperatures from several hundreds to over thousands degrees. The desulfurization is mainly achieved through the sulfation reaction between limestone and SO_2, which is usually the dominant sulfur-baring gas in the flue gases. The limestone can be in calcined or uncalcined state depending on actual reaction conditions. The sulfation reaction between uncalcined limestone and SO_2 is defined as the direct sulfation of limestone, which can be expressed by the following overall reaction:

$$CaCO_3(s) + SO_2(g) + 0.5O_2(g) \rightarrow CaSO_4(s) + CO_2(g) \quad (1)$$

The conditions for this reaction exist in industrial processes such as pressurized fluid-bed combustion (PFBC) and in the preheater tower in cement production.

In cement production, this reaction is one of the key reactions determining the SO_2 emission from the production process. Cement is currently produced mainly by the so-called "dry process." In this process, a cyclone preheater consisting of several cyclones in series (usually 4–5 cyclones) is used to preheat the raw meal (ground raw material mixture) through direct heat exchange between the hot flue gas from the downstream process and the raw meal particles suspended in the gas. In the hot and oxygen-containing environment in the cyclones, SO_2 is formed, mainly from oxidation of pyrite contained in the raw meal. Part of the formed SO_2 is absorbed on the limestone particles—the main constituent

Correspondence concerning this article should be addressed to to G. Hu at this current address: FLSmidth A/S, Vigerslev Allé 77, 2500 Valby, Denmark; e-mail: guh@flsmidth.com.

of the raw meal—through the direct sulfation of the limestone. The rest gets out of the system together with the flue gas. Absorption of SO_2 by the limestone particles in the raw meal in the cyclone preheater is desired for both SO_2 emission reduction from the production process and the production of cement itself because calcium sulfate is a needed minor ingredient of cement products. The residence time of the raw meal particles in each cyclone is relatively short around 10 s.

Hu et al. in their recent studies[1–4] showed that the direct sulfation of limestone in a cyclone preheater-like environment involves oriented nucleation and crystal growth of the solid product—calcium sulfate. Hu et al.[1] suggested that the direct sulfation of limestone may be divided into two distinct periods: the first for the initial sulfation before nucleation of the solid product and the second for the subsequent crystal growth of the solid product, which is partly based on theoretical considerations and partly based on the observed kinetic behavior and product crystal formation during the direct sulfation of limestone. Because of the relatively short residence time of the limestone particles in the cyclone preheater, the kinetics in the first minute which may include both the initial period before nucleation and crystal growth of the solid product and the subsequent period with product crystal growth is important to describe limestone sulfation in the cyclone preheater.

In the past decades, a number of studies[5–18] on the reaction kinetics of the direct sulfation of limestone have been conducted mainly to explore economical and effective methods for SO_2 emission abatement in PFBC. The majority of the earlier works were about limestone sulfation with relatively long durations and high-limestone conversions because of practical reasons of the related applications. Sulfation rate expressions presented in the literature, which generally consider only the influence of SO_2 and temperature, are not able to describe limestone sulfation in the cyclone preheater very well.

The kinetics of the direct sulfation of limestone in the initial period has been studied by Hu et al.[3] in a specially designed flow reactor. In this study, the kinetics of limestone sulfation at the initial stage of the period with product crystal growth is studied in a specially designed fix-bed reactor. The study is going to clarify the kinetics around the transition area from the first period to the second period, which is important for proper simulation of limestone sulfation in the cyclone preheater and for a better understanding of the mechanism of this reaction, as well.

Experimental

Reactor setup

Experiments were performed in a bench–scale quartz fixed-bed reactor. The fixed-bed reactor, as illustrated in Figure 1, was originally developed by Dam-Johansen et al.[19–22] for studying the sulfation of limestone in another context. The reactor consists of a quartz shell and a removable inner tube that contains the sample bed; the inner diameter of the inner tube is 16 mm. The reactor is electrically heated by three separate heating sections. Each of the heating sections has its own temperature controlling system. The reaction temperature is measured by a thermocouple located immediately beneath the sample bed. Temperature mapping of the reactor showed that the temperature variation was less than 2° (K) between the measuring point and the point that is about 10 cm over the bed. It was observed during each experiment that the temperature increased no more than about 0.5°–1° (K) after SO_2 was introduced. The isothermal reaction condition is then considered to be approximately fulfilled.

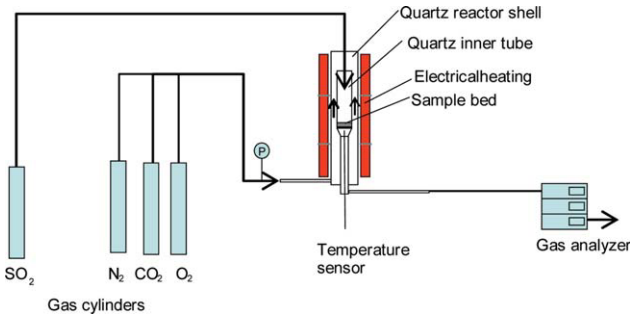

Figure 1. Illustration of the fixed–bed reactor setup.

[Color figure can be viewed in the online issue, which is available at wileyonlinelibrary.com.]

The required gases (SO_2, O_2, CO_2, and N_2) are supplied from gas cylinders with the flow of each gas controlled by a mass flow controller. The gas mixture enters the reactor either at the bottom or at the top and is preheated to the required temperature before it reaches the sample bed. After reaction, the gas mixture flows out of the bottom of the reactor. The gas is then analyzed for SO_2, O_2, and CO_2 by online gas analyzers. The concentrations of SO_2, O_2, and CO_2, temperature, and pressure upstream of the bed are continuously measured and logged via a data acquisition system. More details about performing experiments in this fixed-bed reactor are described in Hu et al.[1]

Limestone sample

The limestone used for the experiments is a soft and porous bryozoan limestone from Faxe Kalk in Denmark (referred to hereafter as Faxe Bryozo). Faxe Bryozo, in powder form when purchased, was sieved by using a standard sieve and the fraction between 0.18 and 0.25 mm was used for the experiments. The limestone particles were dried at about 393 K for 12 h in an electrically heated oven and then stored in air tight containers. Table 1 shows properties of this limestone.

Experimental conditions

The experiments are performed at ambient pressure. The following inlet gas concentrations and temperatures which are relevant values in the cyclone preheater are used: SO_2: 300–1800 ppmv; O_2: 1.5–20 vol %; CO_2: 8–45 vol %; N_2: balance; T: 773–873 K. The sample weight for each experiment is 1 g. The gas flow through the reactor is 1 l/min (at 0.1 MPa and 298 K).

Data deconvolution

Because of residence time distribution (RTD) in the reactor system, the outlet SO_2 concentration measured by the online gas analyzer in the first couple of minutes deviates

Table 1. Properties of Faxe Bryozo

Composition:	
$CaCO_3$ (wt %)	97
Elemental analysis (wt %):	
Na	<Detection limit of 0.001
Mg	0.26
Al	0.026
Si	0.23
P	0.014
S	0.03
K	0.0054
Ca	39
Ti	0.002
V	0.002
Cr	<Detection limit of 0.001
Mn	0.02
Fe	0.047
Zn	0.0014
Sr	0.042
Total surface area (m^2/g)	0.79

significantly from the true SO_2 concentration just after the bed. To assess the true SO_2 concentration just after the bed, the technique of deconvolution was used. The following is a short introduction of this method.[23,24]

Figure 2 illustrates the effect of RTD to outlet concentration. For a vessel with a RTD function of $E(t)$, the outlet concentration profile deviates from the inlet concentration profile in the form of a more flat curve and wider time distribution. The outlet concentration is said to be the convoluted signal of the inlet concentration. The inlet concentration and the outlet concentration are related by the following equation according to the convolution theorem[25]:

$$C_{\text{out}}(t) = \int_0^t C_{\text{in}}(t - t^*)E(t^*)dt^* \tag{2}$$

This equation means: the outlet concentration at time t is the integrated contribution of that part having a residence time of t^* in the input at the inlet at time t^* earlier than t. Equation 2 can be denoted by the following equation:

$$C_{\text{out}} = C_{\text{in}} \times E \tag{3}$$

For the sulfation experiments, the vessel can be considered as the volume from the point just after the bed to the gas analyzer as illustrated in Figure 3. C_{out} is the measured concentration. What needed is C_{in}, the concentration just after the bed without the influence of RTD. The calculation of C_{in} from known C_{out} and E is called deconvolution, which can be done by discrete Fourier transform, as C_{out} and E are usually discrete data series. By performing Fourier transform that is normalized with $N^{-0.5}$ (N: total data points in C_{out} or E) at both sides of Eq. 3, the transformed C_{in} can be calculated by the following equation:

$$F[C_{\text{in}}] = \frac{F[C_{\text{out}}]}{N^{0.5} \times F[E]} \tag{4}$$

C_{in} can then be calculated by perform inverse Fourier transform:

$$F^{-1}[C_{\text{in}}] = F^{-1}\left[\frac{F[C_{\text{out}}]}{F[E]}\right] \times N^{-0.5} \tag{5}$$

The RTD function of the equivalent vessel illustrated in Figure 3 was determined by a step injection of SO_2 gas at the position very close to the bed support filter, which ensures the same vessel properties for the sulfation experiments. Because of the existence of a short period (a few seconds) with full SO_2 absorption at the start of each experiment, steady state above the sample bed was supposed to be established at the moment SO_2 break through the bed. No influence of RTD in the volume from SO_2 injection point to the bed is expected. All experiments were performed with a sampling rate of 2 times per second. Fourier transform calculations were carried out by using Discrete Fourier Transform package in Maple 10 (a mathematical software from MapleSoft). Figure 4 is an example which demonstrates that the

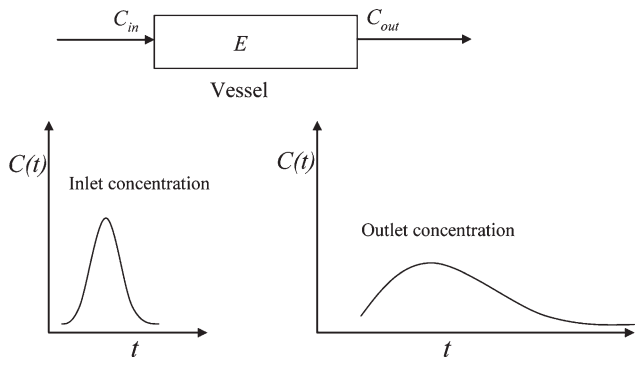

Figure 2. Illustration of the influence of RTD on gas concentration.

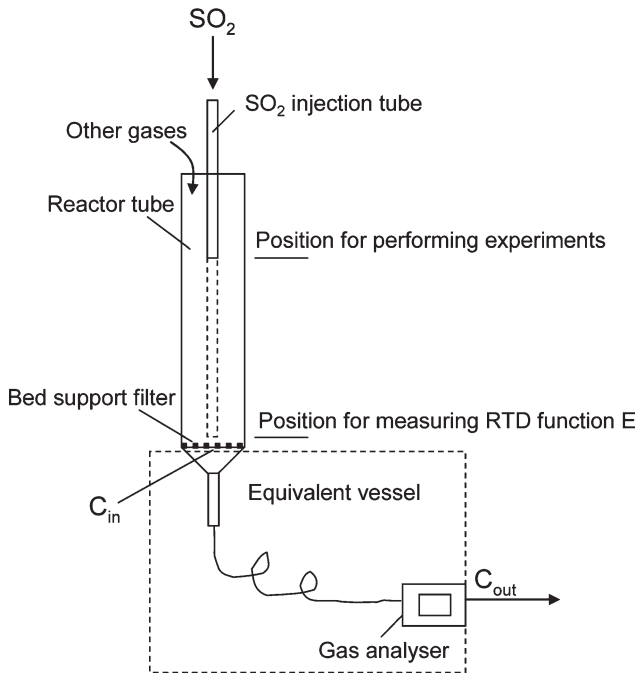

Figure 3. Illustration of the application of deconvolution method in experiments with the fixed–bed reactor.

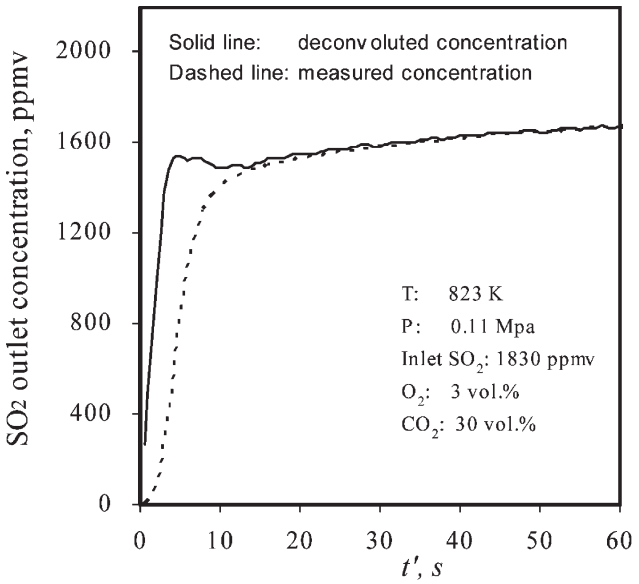

Figure 4. Variation of SO_2 concentration after the bed with and without data deconvolution (reaction conditions: limestone: Faxe Bryozo; *T*: 823 K, *P*: 0.11 MPa; SO_2 (inlet): 1830 ppm SO_2; O_2: 3%; CO_2: 30%; N_2: balance).

influence of RTD at the initial half minute is significant. After this period, the influence of RTD becomes negligible because of the relatively slow increase of SO_2 concentration after the bed. The time scale in Figure 4 is t'—the time from the point where SO_2 is detected by the SO_2 analyzer—instead of the true reaction time t because of the existence of the short period with full SO_2 absorption.

Results and Discussions

The conversion rate of Faxe Bryozo in the initial few minutes were measured by the aforementioned method at different temperatures and gas concentrations. The conversion rate of the limestone sample was calculated based on

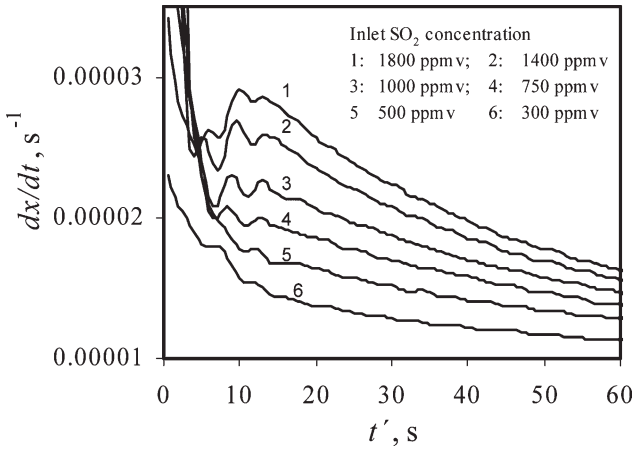

Figure 5. Conversion rate vs. time curves at different SO_2 concentrations at 823 K (other conditions: *P*: 0.11 MPa; O_2: 3%; CO_2: 30%; N_2: balance).

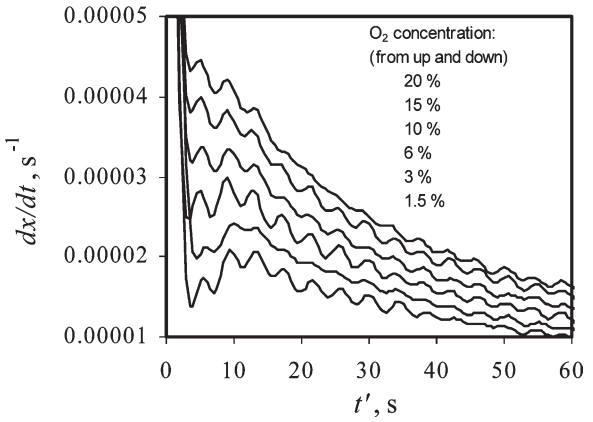

Figure 6. Conversion rate vs. time curves at different O_2 concentrations at 823 K (other conditions: *P*: 0.11 MPa; inlet SO_2: 1800 ppm; CO_2: 30%; N_2: balance).

the difference of SO_2 concentrations before and after the bed by using the following equation:

$$\frac{dx}{dt} = \frac{PV(y_{SO_2,\text{ before the bed}} - y_{SO_2,\text{ after the bed}})M_{CaCO_3}}{RTW\eta}(s^{-1}) \quad (6)$$

The experimental measurement is estimated to have a standard deviation of about ±2.5%, which was evaluated by using the rate data of two set experiments repeated under identical reaction conditions (900 data pairs).

Figures 5–8 show the deconvoluted conversion rate vs. time curves obtained at different gas concentrations and temperatures. These figures show clearly that the conversion rate vs. time curves consist of two parts with widely different kinetic properties: a first part of a few seconds duration with relatively high but fast decreasing conversion rate and a second part with relatively low and slowly decreasing conversion rate. The first part is most likely the ''tail'' of the initial sulfation period, whereas the second part is the initial stage of the period with product crystal growth. Because of the

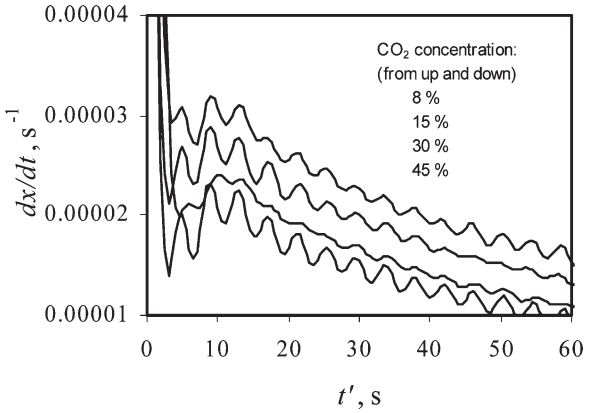

Figure 7. Conversion rate vs. time curves at different CO_2 concentrations at 823 K (other conditions: *P*: 0.11 MPa; inlet SO_2: 1800 ppm; O_2: 3%; N_2: balance).

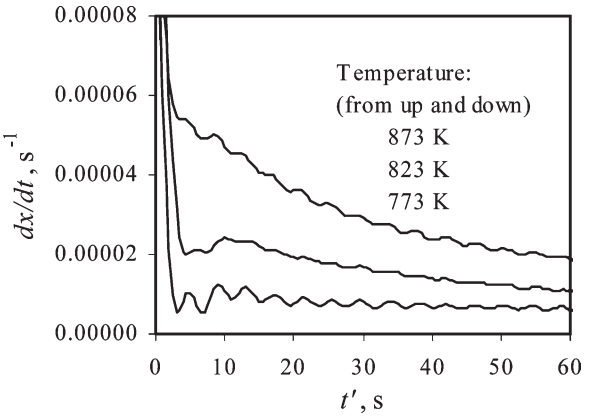

Figure 8. Conversion rate vs. time curves at different temperatures (other conditions: *P*: 0.11 MPa; inlet SO_2: 1800 ppm; O_2: 3%; CO_2: 30%; N_2: balance).

fast initial sulfation rate, a short period of a few seconds with full absorption was present for all the experiments. This short period with full absorption at the start is the reason for that the other part of the initial sulfation period can not be measured here. The initial kinetics of the direct sulfation of Faxe Bryozo has been presented by Hu et al.,[3] and therefore, will not be discussed again in this article. The second part of the conversion rate vs. time curves will be the focus of this article.

As shown in Figures 5–8, small fluctuations appears at the sharp transition from the first period to the second period in some of the conversion rate vs. time curves. The fluctuations seem to become less significant with increasing temperature, increasing O_2 concentration, and decreasing SO_2 and CO_2 concentrations. It is not clear whether this fluctuation is caused by the deconvolution or by other reasons. In these figures, t', the reaction time starting from the moment at which SO_2 breaks through the sample bed is used in stead of the total reaction time.

Figures 5–8 demonstrate that the sulfation reaction at the initial stage of the period with product crystal growth is significantly promoted by higher SO_2 concentrations, higher O_2 concentrations, lower CO_2 concentrations, and higher temperatures, respectively. Figure 6 demonstrates that O_2 has significant influence on the reaction even at a concentration of 20%, which is different from the zero-order behavior of O_2 observed by Hu et al.[1] at similar concentration but with a few minutes longer reaction time.

The change of the effect of O_2 with the reaction time can be explained by the sulfation mechanism proposed by Hu et al.,[1,3] which suggests that SO_2 molecules are first absorbed at the active sites at the calcite surface and are then converted to sulfite ions. The formed sulfite ions are thereafter oxidized to form sulfate ions. After the sulfate ion concentration at the surface reaches the critical level, nucleation and crystal grain growth of the solid product—anhydrite takes place. As observed by Hu et al.,[1,4] the nucleation and crystal grain growth of the solid product are oriented. The crushed calcite particles contain cleavages and fractures. This oriented nucleation and crystal grain growth of the solid product takes place only at the fractures along the lattice plane {1,0,4} of calcite because of the good match of crystal lattice structure at this specific lattice plane between calcite and anhydrite. Initially, because of the relatively fast diffusion of the formed sulfate ion at the calcite surface[3] to the growing anhydrite crystals, the active sites are quickly released and available for the absorption of SO_2 and the subsequent formation of sulfite again. At this period, oxygen concentration shows significant influence on the apparent sulfation rate because of the presence of significant amount of sulfite ions. However, with the progress of the sulfation process, the very reactive calcite fractures are gradually covered by the growing anhydrite crystals. The apparent sulfation rate decreases significantly. The slow down of the sulfation rate is mainly caused by two reasons. One is the disappearing of the more reactive fracture surface area. The second is the increasing resistance of solid-state diffusion because of the increasing thickness of the product crystal layer, which means also a slower release of the active sites for further reaction. Because of these two reasons, the sulfite ion concentration at the calcite and product surface is significantly reduced. At the point where the sulfite ion concentration approaches zero, the influence of O_2 concentration will show zero-order effect. Conditions that can have influence on the sulfation rate and solid-state diffusion, such as gas composition, temperature level, limestone conversion, and additives[2] will have influence on the effect of O_2 concentration.

As demonstrated in Figures 5–8, the transition from the first period to the second period is rather sharp. The conversion rate at the transition point, $(dx/dt)_g$ seems to be a characteristic property of limestone sulfation. To assess the values of $(dx/dt)_g$ at different reaction conditions, a plot of $(dx/dt)_g$ (in logarithmic scale) against limestone conversion x is made for each experiment, because it was observed in all the experiments carried out in this study that there is a good linear relationship between $\ln((dx/dt)_g)$ and limestone conversion in the initial stage of the second period. The values of $(dx/dt)_g$ at different conditions can be read directly from the plots. For these curves with small fluctuation in the transition area, the $(dx/dt)_g$ is obtained by a limited extrapolation as illustrated in Figure 9.

Figures 10–12 show the obtained values of $(dx/dt)_g$ at different SO_2, O_2, and CO_2 concentrations and different temperatures. As seen in these figures, there are good correlations between $(dx/dt)_g$ and the gas concentrations and the temperature. $(dx/dt)_g$ increases with increasing SO_2 and O_2 concentrations and increasing temperature, but decreases with increasing CO_2 concentration. With the obtained values of $(dx/dt)_g$ at different inlet SO_2 concentrations, the corresponding outlet SO_2 concentrations and the average SO_2 concentrations in the limestone sample bed are thus calculated. By using the average SO_2 concentrations, the apparent reaction orders of SO_2, O_2, and CO_2 at the transition point are calculated to be $\sim$0.6, 0.4, and $-$0.2, respectively. The apparent activation energy is calculated to be $\sim$105 kJ/mol.

By comparing the obtained apparent reaction orders of 0.2, 0.2, and $-$0.5 for SO_2, O_2, and CO_2, respectively, and an activation energy of 104 kJ/mol for the sulfation reaction after longer reaction time[1] with the above values obtained for $(dx/dt)_g$, it can be seen that the influences of the SO_2,

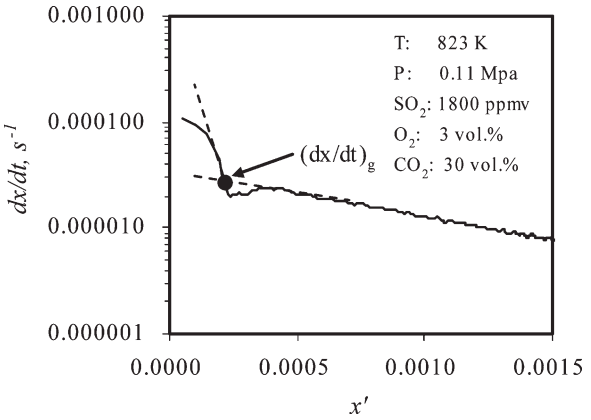

Figure 9. Illustration of plot of ln(*dx*/*dt*) against *x*′.

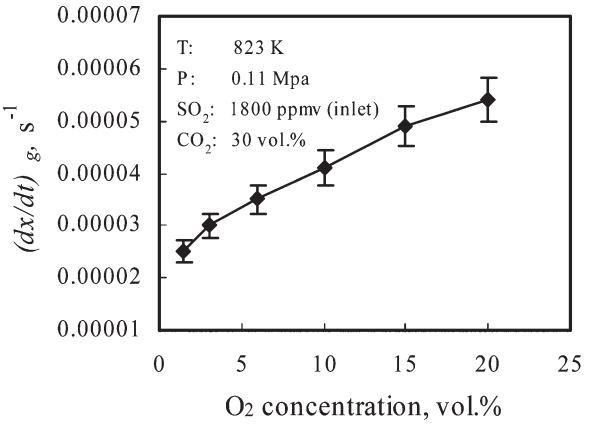

Figure 11. Variation of $(dx/dt)_g$ with O_2 concentration for Faxe Bryozo.

O_2, CO_2, and temperature are quite similar. This seems to be quite reasonable result considering that the transition point is actually the start point for the period with crystal growth of the solid product. However, the magnitudes of these values are not comparable because the conditions for the evaluation of these values are not the same.

The variation of limestone conversion rate with increasing limestone conversion after the transition point is reflected by the slope of the plot of $\ln((dx/dt)_g)$ against x. Plots of $\ln((dx/dt)_g)$ against x at different gas concentrations and temperature shows that this slope (absolute value) decreases with increasing temperature, increasing O_2 concentration and decreasing CO_2 concentration. SO_2 showed no influence. The variation of this slope with O_2 and CO_2 concentrations was evaluated to correspond to the powers of -0.12 and 0.4, respectively. The influence of temperature on this slope, when evaluated according to an expression of the form as Arrhenius equation, corresponds to an exponential constant of -45 kJ/mol.

The variation of this slope with the temperature and O_2 and CO_2 concentrations may be related to the growth of the product crystals. The increase of the slope with decreasing temperature is probably due to the formation of more nuclei at lower temperatures,[26] which results in coverage of more calcite surface area with the same amount of solid product. The slope increases with increasing CO_2 concentrations probably due to the same reason for the influence of temperature, as a significant increase in solid-state diffusion resistance at higher CO_2 concentrations[27,28] may cause formation of more nuclei as well.

The effect of O_2 on the slope may be related to its influence on the formation of sulfite ions. With the growth of the solid product grains, carbonate ion concentration at the calcite surface may increase because of the shorter diffusion distance of sulfate ions, which compensates partly for the effect of reduced calcite surface area. The relative decrease in the conversion rate becomes smaller if the relative increase in the carbonate ion concentration is larger. With decreasing O_2 concentration, sulfite concentration at the calcite surface may increase, which makes the increase in carbonate ion concentration by the shortened diffusion distance less significant and thus causes a larger decrease in conversion rate with increasing conversion.

Modeling

As mentioned in the introduction, the direct sulfation of limestone involves oriented nucleation and growth of the product crystals. At the initial stage of the period with product crystal growth, the calcite surface is gradually covered by the growing product crystals as illustrated in Figure 13.

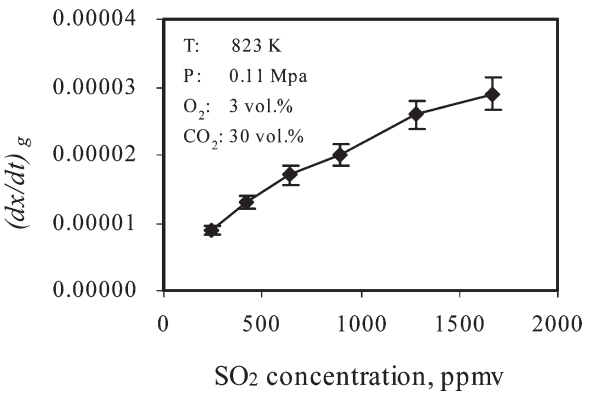

Figure 10. Variation of $(dx/dt)_g$ with SO_2 concentration for Faxe Bryozo.

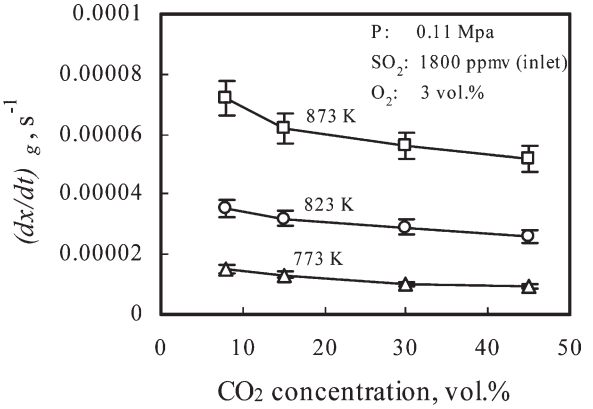

Figure 12. Variation of $(dx/dt)_g$ with CO_2 concentration at different temperatures for Faxe Bryozo.

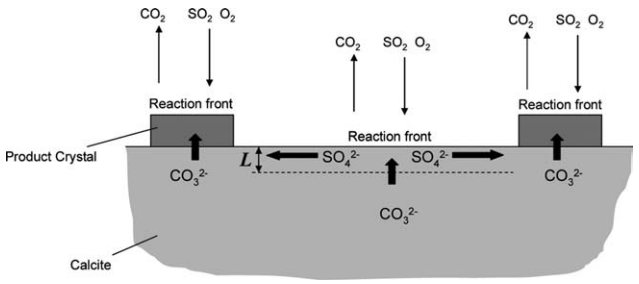

Figure 13. Illustration of the sulfation process in the period with product crystal growth.

The conversion rate of the limestone contains contributions from both the sulfation reaction at the calcite surface and the sulfation reaction at the surface of the product crystals. This can be expressed by the following general expression:

$$\frac{dx}{dt} = r_c s_c + r_p s_p \tag{7}$$

Here, subscripts c and p means calcite and product crystal, respectively.

However, the reaction rate at the surface of the product crystals is much lower than the reaction rate at the calcite surface because of much higher resistance of solid-state diffusion through the crystals of the product. In the initial stage of the period with product crystal growth, the contribution from the reaction at the product crystal surface is relatively small and thus can be neglected.

Hu et al.[3] proposed a reaction-diffusion mechanism for the initial sulfation process at the calcite surface before nucleation of the solid product. According to this mechanism, the sulfation reaction takes place at the calcite surface. The formed product ions (sulfate and sulfite) diffuse toward the inner part of the calcite grain, whereas the carbonate ions diffuse from the inner part of calcite grain to the surface to participate the reaction. They established the following mathematical model to describe this reaction-diffusion process:

$$\frac{\partial a(l,t)}{\partial t} = D_s \frac{\partial^2 a(l,t)}{\partial l^2} \tag{8}$$

$$\text{IC1} : a(l,0) = 1 \tag{9}$$

$$\text{BC1} : a(l,t) = 1 \quad \text{when } l \to \infty \tag{10}$$

$$\text{BC2} : \frac{\partial a(0,t)}{\partial l} = \left(\frac{1}{D_s C^0_{CO_3^{2-}}}\right) r^0 a(0,t) \tag{11}$$

This model is supposed to be valid here as well for the reaction at calcite surface. However, due to the growth of product crystals, the product ions—sulfate ions now diffuse toward the product crystals in a thin layer at the calcite surface instead of diffusing towards the inner part of the calcite grain. This means that BC1 now can be changed to as the following equation:

$$\text{BC1} : a(l,t) = 1 \quad \text{when } l \to L \tag{12}$$

At constant or slow varying gas concentrations, quasi-stead-state for the diffusion of carbonate ions across this thin layer at the surface of the calcite grain can be assumed. With these assumptions, the equation systems consisting of Eqs. 8, 9, 11, and 12 can be solved to get the following expression for carbonate ion concentration at the calcite surface:

$$a^s = \frac{1}{1+\psi} \tag{13}$$

Here $\psi = \frac{r^0 L}{D_s C^0_{CO_3^{2-}}}$, a parameter indicating the relative rate of chemical reaction against solid-state diffusion.

Now Eq. 7 can be reformulated as follows:

$$\frac{dx}{dt} = r^0 a^s s_c = \frac{r^0}{1+\psi} s_c \tag{14}$$

The free calcite surface area S_c decrease with increasing conversion and can be described as a function of limestone conversion. Equation 14 can thus be rewritten as follows:

$$\frac{dx}{dt} = \frac{r^0}{1+\psi} s_c^t f(x) \tag{15}$$

To use Eq. 15 to describe the variation of limestone conversion rate, it is necessary to know the values of effective layer thickness for the diffusion, L and the function $f(x)$ that describes the loss of calcite surface area. Unfortunately, the experimental data obtained in this study is not sufficient to assess these parameters.

However, as shown earlier, for the experiments carried out in this study, the conversion rates at the transition point from the first period to the second period can be assessed. Further more, a good linear relationship between $\ln(dx/dt)$ and limestone conversion exists in the initial stage of the second sulfation period. Equation 15 can now be written as follows by using these properties:

$$\frac{dx}{dt} = \left(\frac{dx}{dt}\right)_g e^{-Bx''} \tag{16}$$

Here, $\left(\frac{dx}{dt}\right)_g = \frac{r^0}{1+\psi} s_c^g$; x'' is the increase in limestone conversion from the start of the second period.

Integration of Eq. 16 gives the following equation for the conversion of limestone as a function of reaction time:

$$x'' = \left(\frac{1}{B}\right) \ln\left(1 + B\left(\frac{dx}{dt}\right)_g t''\right) \tag{17}$$

By using the apparent reaction orders and activation energy evaluated earlier for the variation of $(dx/dt)_g$ with the concentrations of SO_2, O_2, and CO_2 and the reaction temperature, the following expression for $(dx/dt)_g$ is obtained:

$$\left(\frac{dx}{dt}\right)_g = 2165\, e^{\frac{-105{,}000}{\Re T}} C^{0.6}_{SO_2} C^{0.4}_{O_2} C^{-0.2}_{CO_2} \tag{18}$$

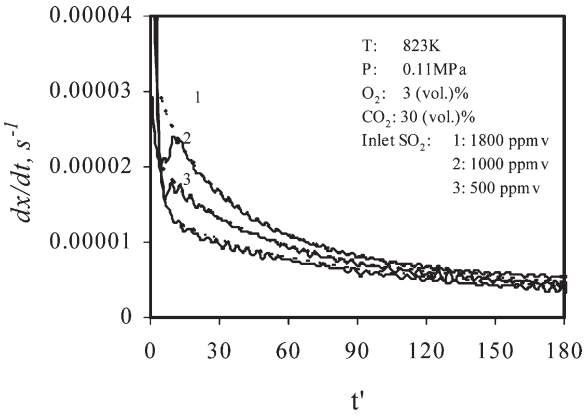

Figure 14. Comparison between the measured conversion rate of Faxe Bryozo and the model predicted values at 823 K and different SO_2 concentrations (solid lines: experimental results; dashed lines: model simulations).

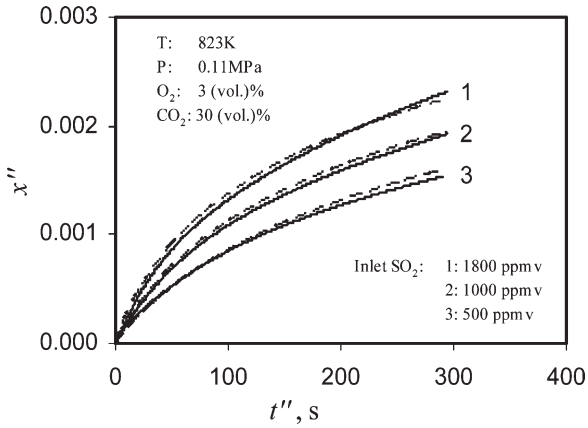

Figure 16. Comparison between the measured conversion of Faxe Bryozo and the model predicted values at 823 K and different SO_2 concentrations (solid lines: experimental results; dashed lines: model simulations).

The parameter B is the slope of the plot of $\ln(dx/dt)$ against x''. The influence of the concentrations of SO_2, O_2, and CO_2 and the reaction temperature on parameter B has been evaluated earlier. By using these values, the following equation for B is obtained:

$$B = 0.73\, e^{\frac{44{,}800}{\Re T}}\, C_{O_2}^{-0.12}\, C_{CO_2}^{0.4}\,(\text{Dimensionless}) \qquad (19)$$

By using Eqs. 17–19, limestone conversion rate and the increase in limestone conversion after the start point of product crystal growth can be calculated. Figures 14–17 show comparisons between experimental data and model simulations. Figures 14 and 15 show the comparison between the measured conversion rate vs. time curves and the model simulated curves, whereas Figures 16 and 17 show the comparison between the measured conversion vs. time curves and the model simulated curves. As seen in these figures, the model generally follows the sulfation process quite well up to x'' around 0.3% (the total conversion is estimated to be roughly 0.4–0.5%). The model undershoots at higher limestone conversions.

The general undershot by the model at higher limestone conversions may be explained by several reasons. First, the loss of the calcite surface area may not continue at the same pattern when the conversion increases to a relatively high level. Hu et al.[1] showed that even when the calcite grain surface is fully covered by the product crystals voids are still present because of the different orientations of the product crystal grains with Faxe Bryozo. The second is that the sulfation reaction at the surface area of the product crystals may become significant relative to the sulfation reaction at the surface area of the calcite grain when the calcite surface area is reduced to a very low level. The effective layer thickness for the diffusion of carbonate ions may vary as well with increasing conversion. For the simulation of the

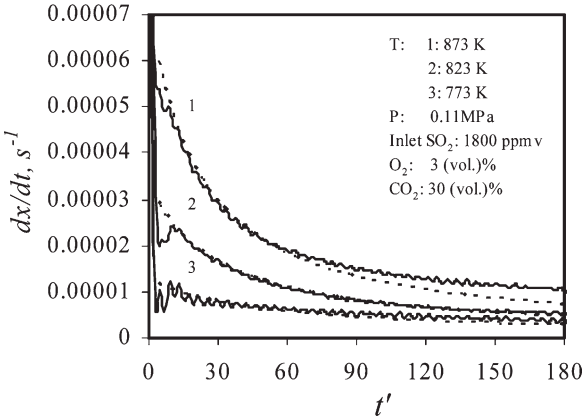

Figure 15. Comparison between the measured conversion rate of Faxe Bryozo and the model predicted values at different temperatures (solid lines: experimental results; dashed lines: model simulations).

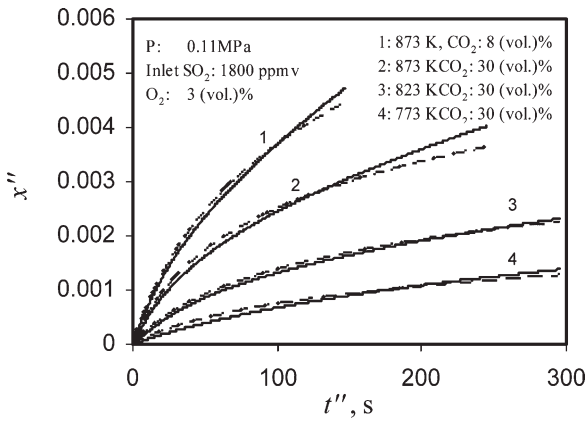

Figure 17. Variation of conversion of Faxe Bryozo with reaction time at different temperatures (solid lines: experimental results; dashed lines: model simulations; 1: 873 K, 8% CO_2; 2: 873 K, 30% CO_2; 3: 823 K; 4: 773 K. Other conditions if not specified: P: 0.11 MPa; SO_2: 1800 ppm; O_2: 3%; CO_2: 30%; N_2: balance).

sulfation reaction at conversion higher than around 0.5%, more sophisticated models is therefore needed.

It needs to be pointed out here that the direct sulfation of limestone is a complicated reaction. The apparent reaction orders of the gases, the apparent activation energy, and the product layer structure all vary with reaction conditions.[29] The model established above is, therefore, not supposed to be able to simulate limestone sufation at very different conditions, such as at much higher temperatures or gas concentrations than the temperatures and gas concentrations used in this study. A typical example is the influence of oxygen. It is expected that the apparent reaction order of oxygen may become zero at certain concentration level. Faulty results will thus be inevitable if this is not considered.

Conclusions

This study, through the application of data deconvolution, demonstrates clearly that the direct sulfation of limestone has a two-period kinetic behavior: a short initial sulfation period before nucleation of the solid product with high but fast decreasing reaction rate and a subsequent period with product crystal growth with low but slow decreasing conversion rate. The relatively slow decrease in the conversion rate of limestone in the period with product crystal growth is mainly because of the relatively slow covering of the calcite surface area by crystals grains of the solid product. The transition from the first period to the second period is sharp and is clearly reflected in the limestone conversion rate vs. reaction time or limestone conversion curves of the sulfation process. The transition point in a limestone conversion rate vs. reaction time or limestone conversion curve is determined by the gas concentrations and the temperature.

At the initial stage of the second period with product crystal growth and at the reaction conditions used in this study, the sulfation of Faxe Bryozo is under mixed control by both chemical reaction and solid-state diffusion. The observed kinetic behavior of the sulfation process in the period with product crystal growth can be explained by the combination of the sulfation reaction at the gas–solid interface, diffusion of the product ions toward the product crystal grains, diffusion of carbonate ions toward the gas–solid interface to participate the reaction, and the gradual shielding of calcite surface area by the product crystal grains.

A semi-theoretical model based on the reaction-diffusion theory and the growth of the solid product is established. The model gives a satisfactory description of the sulfation process of Faxe Bryozo at conversion levels lower than around 0.5%.

Acknowledgments

This work is part of the CHEC (Combustion and Harmful Emission Control) Research Center funded a.o. by the Technical University of Denmark, the Danish Technical Research Council, the European Union, the Nordic Energy Research, Dong Energy A/S, Vattenfall A.B., FLSmidth A/S, and Public Service Obligation funds from Energinet.dk and the Danish Energy Research program. This work is financially supported by FLSmidth A/S and the Technical University of Denmark.

Notation

a = ratio between actual carbonate ion concentration and carbonate ion concentration in pure calcite, dimensionless
B = constant, dimensionless
C = concentration, mol/m^3
D = diffusion coefficient, m^2/s
E_a = activation energy, J/mol
M = molar weight
P = total pressure
p = partial pressure
R = gas constant
s = surface area, m^2/mol
r = surface reaction rate, mol/(m^2 s)
t = reaction time, s
T = temperature, K
V = gas flow, m^3/s
W = sample weight, g
x = conversion of limestone, dimensionless
y = molar fraction, dimensionless
η = fraction of $CaCO_3$ in limestone
ψ = dimensionless modulus

Superscript

0 = intrinsic
s = surface
t = total

Subscript

g = growth
c = calcite
p = product
s = solid-state

Literature Cited

1. Hu G, Dam-Johansen K, Wedel S, Hansen JP. Direct sulfation of limestone. *AIChE J*. 2007;53:958–960.
2. Hu G, Dam-Johansen K, Wedel S, Hansen JP. Enhancement of the direct sulfation of limestone by alkali metal salts, calcium chloride, and hydrogen chloride. *Ind Eng Chem Res*. 2007;46:5295–5303.
3. Hu G, Dam-Johansen K, Wedel S, Hansen JP. Initial kinetics of the direct sulfation of limestone. *AIChE J*. 2008;54:2663–2673.
4. Hu G, Dam-Johansen K, Wedel S. Oriented nucleation and growth of anhydrite during direct sulfation of limestone. *Cryst Growth Des*. 2008;8:1181–1185.
5. Snow MJH, Longwell JP, Sarofim AF. Direct sulfation of calcium carbonate. *Ind Eng Chem Res*. 1988;27:268–273.
6. Hajaligol MR, Longwell JP, Sarofim AF. Analysis and modeling of the direct sulfation of $CaCO_3$. *Ind Eng Chem Res*. 1988;27:2203–2210.
7. Iisa K, Hupa M, Yrjas P. Product layer diffusion in the sulfation of calcium carbonate. In: *24th Symposium (International) on Combustion*. The Combustion Institute, Pittsburgh, 1992:1349–1356.
8. Iisa K, Hupa M. Rate–limiting processes for the desulfurization reaction at elevated pressures. *J Inst Energy*. 1992;65:201–205.
9. Fuertes AB, Velasco G, Fuente E, Parra JB, Alvarez T. Sulfur retention by limestone particles under PFBC conditions. *Fuel Process Technol*. 1993;36:65–71.
10. Fuertes AB, Velasco G, Fuente E, Alvarez T. Study of the sulfation of limestone particles at high CO_2 partial pressure. *Fuel Process Technol*. 1994;38:181–192.
11. Illerup JB, Dam-Johansen K, Lunden K. High–temperature reaction between sulfur dioxide and limestone. VI. The influence of high pressure. *Chem Eng Sci*. 1993;48:2151–2157.
12. Krishnan SV, Sotirchos SV. Sulfation of high purity limestones under simulated PFBC conditions. *Can J Chem Eng*. 1993;71:244–255.
13. Tullin C, Nyman G, Ghardashkhani S. Direct sulfation of $CaCO_3$: the influence of CO_2 partial pressure. *Energy Fuels*. 1993;7:512–519.
14. Zhong Q. Direct sulfation reaction of SO_2 with calcium carbonate. *Thermochim Acta*. 1995;260:125–136.
15. Zevenhoven R, Yrjas P, Hupa M. Sulfur dioxide capture under PFBC conditions: the influence of sorbent particle structure. *Fuel*. 1998;77:285–292.

16. Alvarez E, Gonzalez JF. High pressure thermogravimetric analysis of the direct sulfation of Spanish calcium–based sorbents. *Fuel*. 1999;78:341–348.
17. Liu H, Katagiri S, Kaneko U, Okazaki K. Sulfation behaviour of limestone under high CO_2 concentration in O_2/CO_2 coal combustion. *Fuel*. 2000;79:945–953.
18. Qiu K, Lindqvist O. Direct sulfation of limestone at elevated pressures. *Chem Eng Sci*. 2000;55:3091–3100.
19. Dam-Johansen K, Østergaard K. High–temperature reaction between sulfur dioxide and limestone. I. Comparison of limestone in two laboratory reactors and a pilot plant. *Chem Eng Sci*. 1991;46:827–837.
20. Dam-Johansen K, Østergaard K. High–temperature reaction between sulfur dioxide and limestone. II. An improved experimental basis for a mathematical model. *Chem Eng Sci*. 1991;46:839–845.
21. Dam-Johansen K, Hansen PFB, Østergaard K. High–temperature reaction between sulfur dioxide and limestone. III. A grain–micrograin model and its verification. *Chem Eng Sci*. 1991;46:847–853.
22. Dam-Johansen K, Østergaard K. High–temperature reaction between sulfur dioxide and limestone. IV. *Chem Eng Sci*. 1991;46:855–859.
23. Levenspiel O. *Chemical Reaction Engineering*. New York: Wiley, 1999.
24. Jensen LS. NO_x from cement production—reduction by primary measures. PhD Thesis. Dept. of Chemical and Biochemical Engineering, Technical University of Denmark, Lyngby, Denmark, 1999.
25. Varma A, Morbidelli M. *Mathematical Methods in Chemical Engineering*. New York: Oxford University Press, 1997.
26. Duo W, Laursen K, Lim J, Grace J. Crystallization and fracture: formation of product layers in sulfation of calcined limestone. *Powder Technol*. 2000;111:154–167.
27. Beruto D, Giordani M, Botter R. Microstructure development of Li_2CO_3–$CaCO_3$ eutectic mixture in CO_2 (g) and N_2 (g) environment. *J Phys Coll*. 1986;47(Suppl 2):C1527–C1531.
28. Tetard F, Bernache-Assollant D, Champion E. Pre–eutectic densification of calcium carbonate doped with lithium carbonate. *J Therm Anal Calorim*. 1999;56:1461–1473.
29. Hu G, Dam-Johansen K, Wedel S, Hansen JP. Review of the direct sulfation reaction of limestone. *Prog Energy Combust Sci*. 2006;32:386–407.

Manuscript received Jan. 17, 2010, and revision received Jun. 26, 2010.